Characterization of microtubule associated protein tau isoforms and Alzheimer's disease-like pathology in normal sheep (*Ovis aries*) - relevance to their potential as a model of Alzheimer's disease.

Emma S. Davies (esd5@aber.ac.uk)
Aberystwyth University - Penglais Campus: Aberystwyth University https://orcid.org/0000-0003-1149-9233

Russel M. Morphew
IBERS: Aberystwyth University Institute of Biological Environmental and Rural Sciences

David Cutress
IBERS: Aberystwyth University Institute of Biological Environmental and Rural Sciences

A. Jennifer Morton
Cambridge University: University of Cambridge

Sebastian McBride
IBERS: Aberystwyth University Institute of Biological Environmental and Rural Sciences
https://orcid.org/0000-0001-5120-0115

Research Article

Keywords: Alzheimer's disease, amyloid-β, MAPT, tau, isoform expression, sheep

Posted Date: March 10th, 2022

DOI: https://doi.org/10.21203/rs.3.rs-1419996/v1

Abstract

Alzheimer's disease is a chronic neurodegenerative disease that accounts for up to 80% of all dementias. Characterised by deteriorations of memory and cognitive function, the key neuropathological features are accumulations of β-amyloid and hyperphosphorylated tau, as 'plaques' and 'tangles' respectively. Despite extensive study, however, the exact mechanism underlying aggregate formation in Alzheimer's disease remains elusive, as does the contribution of these aggregates to disease progression. Importantly, a recent evaluation of current Alzheimer's disease animal models suggested that rodent models are not able to fully recapitulate the pathological intricacies of the disease as it occurs in humans. Therefore, increasing attention is being paid to species that might make good alternatives to rodents for studying the molecular pathology of Alzheimer's disease. The sheep (*Ovis aries*) is one such species, although to date there have been few molecular studies relating to Alzheimer's disease in sheep. Here, we investigated the Alzheimer's disease relevant histopathological characteristics of twenty-two sheep, using anti-β-amyloid (Abcam 12267 and mOC64) and phosphorylation specific anti-tau (AT8 and S396) antibodies. We identified numerous intraneuronal aggregates of both β-amyloid and tau that are consistent with early Alzheimer's disease-like pathology. We confirmed the expression of two 3-repeat (1N3R, 2N3R) and two 4-repeat (1N4R, 2N4R) tau isoforms in the ovine brain, which result from the alternative splicing of two tau exons. Finally, we investigated the phosphorylation status of the serine396 residue in thirty sheep, and report that the phosphorylation of this residue begins in sheep aged as young as two years. Together, these data show that sheep exhibit naturally occurring β-amyloid and tau pathologies, that reflect those that occur in the early stages of Alzheimer's disease. This is an important step towards the validation of the sheep as a feasible large animal species in which to model Alzheimer's disease.

1.0 Introduction

Alzheimer's disease (AD) is a progressive neurodegenerative disease that presents with debilitating memory and cognitive impairments, and accounts for between 60–80% of all dementias worldwide [92]. Whilst the prevalence and the consequent economic and social impacts of AD are predicted to increase each year as the global population ages, the exact aetiology of AD is still unknown, making the development of effective treatments extremely challenging [19]. Accumulations of β-amyloid (Aβ) exhibited as extracellular plaques and cerebral amyloid angiopathy (CAA), and accumulations of hyperphosphorylated tau present as paired helical filaments (PHFs) and neurofibrillary tangles (NFTs) are accompanied by significant neuronal loss and constitute the primary histopathological hallmarks of the disease [11, 19].

Rodents do not naturally exhibit either Aβ or tau pathology as they age [25]. This presents a particular challenge when using rodents as a species for preclinical studies. To overcome this obstacle, it has been necessary to create transgenic mouse models overexpressing Aβ [63]. Such models have been used to elucidate the significance of mutations in the amyloid precursor (APP), and presenilin proteins (PSEN1 and PSEN2) that cause familial AD (FAD) [25]. Mutations in these proteins affect APP metabolism, leading to an increased production of the amyloidogenic form of Aβ (Aβ-42), and impaired Aβ clearance

[36]. These events form the basis of the 'amyloid cascade hypothesis' to explain the pathogenesis of AD, in which it is proposed that accumulation of Aβ-42 is the primary pathological event that drives all other associated pathologies (including tau pathology, inflammation, vascular damage, and neuronal loss) [36]. This hypothesis, however, does not explain the mechanisms by which soluble and/or insoluble forms of intracellular and/or extracellular aggregates of Aβ and tau differentially affect one another [47, 68]. Indeed, while transgenic mouse models using APP and PSEN mutations present with significant Aβ pathology between three and six months of age they often fail to exhibit significant tau pathology or neuron loss [25]. Consequently, tau pathologies within these rodent models are achieved only by introducing tau mutations that cause tau pathology in other dementias, namely those associated with frontotemporal dementia with parkinsonism-17 (FTDP-17) [25]. This, combined with the relatively short lifespan of rodents means that the capacity of transgenic mouse models to fully reflect the aetiological mechanisms and temporal progression of familial AD is limited [74]. Furthermore, given the lack of naturally occurring age-related neuropathology, the ability of mouse models to recapitulate mechanisms associated with 'sporadic' AD (that is not associated with mutations in any of the FAD genes and accounts for more than 95% of AD cases), is also extremely restricted [21].

Increasing recognition of the limitations associated with rodent models of AD has led to the investigation of species that have a longer lifespan, a more physically and functionally differentiated brain, and a propensity to naturally develop both Aβ and tau pathology with age [22, 73]. Non-human primates such as the chimpanzee (*Pan troglodytes*), rhesus macaque (*Macaca mulatta*) and common marmoset (*Callithrix jacchus*) are of particular interest because they naturally develop some AD-like pathology [38]. For example, diffuse and dense-cored Aβ plaques, and CAA have been detected in aged chimpanzees [24, 26, 28, 71], rhesus macaques [72, 88] and marmosets [33, 54], with quantities of Aβ in aged individuals comparable to levels seen in AD patients. NFTs have also been described within the entorhinal cortex of aged chimpanzees and rhesus macaques [4], while in marmosets, abnormally phosphorylated tau has been identified as early as adolescence [70]. Other species that exhibit AD-like pathology include the domestic dog (*Canis familiaris*) [16, 17, 73, 79] and cat (*Felis catus*) [12]. Both dogs and cats develop cognitive decline alongside diffuse Aβ plaques in old age, however, tau pathology rarely accompanies Aβ deposition and dense-cored Aβ plaques and NFTs are not consistently detected. Whilst these species have the potential to mitigate the limitations of current rodent AD models, they are limited in terms of their ethical use and therefore their numbers available to facilitate robust experimental design.

We chose to focus on sheep as a potential animal model of human AD for a number of reasons. Sheep have a moderate lifespan (fifteen-twenty years), an extensively annotated reference genome [46], are numerous within a well-established agricultural production infrastructure, and can be kept in a naturalised environment. Sheep also have a highly gyrencephalic neocortex with differentiated cortical and subcortical structures [57]. This species has also been used as a model for studying the neurodevelopmental and cognitive effects of hormone manipulation [42, 69], Huntington's disease [43, 58, 59, 78], and Batten disease [6, 23, 75]. Sheep between eight and fourteen years of age have also been shown to spontaneously develop both diffuse Aβ plaques [67] and NFTs [7, 60, 61]. These findings were confirmed in a pilot study (within this study) and suggest that sheep could provide a more robust model

of AD than species that do not naturally develop this pathology. While these studies point towards sheep as a potential AD model, few molecular studies of AD-relevant proteins have been conducted in sheep in order to fully assess the translatability of the model. For example, whereas humans express six central nervous system (CNS) tau isoforms formed from the alternative splicing of three exons, the tau isoform expression of sheep has been predicted but not confirmed experimentally [44, 62]. Furthermore, whilst in humans over seventy different possible phosphorylation sites of the tau protein have been identified and associated with different time points of AD progression [86], similar information (that may be critical in identifying early tau dysfunction during AD aetiology) is extremely limited in the ovine model [7, 60, 61]. The aims of this study, therefore, were to characterise Aβ and tau histopathology, including tau phosphorylation, in sheep of a range of ages, and to investigate the nature of tau isoform expression in sheep. The results of the aforementioned pilot study are also described.

2.0 Methods

2.1 Pilot Experiment

The methodology of the pilot study which examined the brains of two sheep, one 21 years of age (P1), and one 16 years of age (P2) is described within the supplementary material (Online Resource 1). These sheep had been euthanised by a veterinary surgeon for humane reasons and their brains were donated by the owner.

2.2 Main study sheep

A total of 30 sheep brains, obtained as by-products from commercial sheep intended for human consumption (hereafter called stock sheep) were examined in this study. All of these sheep were killed by electrical stunning and exsanguination. The breed of each animal was recorded and its age (determined via dentition [15]) was estimated at the point of sample collection. Sheep were judged to be purebred (Cheviot $n = 1$, Southdown $n = 1$, Herdwick $n = 1$), Mule ($n = 15$), or Texel cross ($n = 12$). All but one of the sheep were female. Sheep were estimated to be 1–2 years of age ($n = 10$), 2–3 years of age ($n = 10$), and > 5 years of age ($n = 10$).

2.3 Histopathology

Twenty brains (from stock sheep aged 1–2 and > 5 years of age) were examined histologically. Following extraction, the right brain hemisphere was dissected, snap frozen, and stored at -80°C until use. The left brain hemisphere was fixed in 10% neutral-buffered formalin (4% v/v formaldehyde) for four days, dissected into coronal blocks and post-fixed for a further three days. Fixed tissue was dehydrated and embedded in paraffin wax, cut into 4 µm thick sections, mounted onto slides, and dried at 45 ℃ overnight, before being bonded at 70 ℃ for one hour. Sections were stained using haematoxylin and eosin (CellPath). Additional 4 µm thick human hippocampal tissue samples were obtained from the Medical Research Council UK Brain Bank Network to provide human AD positive and AD negative control samples.

2.4 Immunohistochemistry

Immunohistochemistry was performed using a labelled streptavidin-biotin method. Wash steps between incubations were conducted using tris buffered saline (TBS). Briefly, following deparaffinisation and rehydration, antigen retrieval was performed by incubating sections in 95% v/v formic acid for 20 minutes (RT). The sections were incubated in 5% v/v normal goat serum (Merck, S26-100) with 1% w/v BSA protein block for 2 hours (RT) to prevent non-specific binding. Streptavidin and biotin blocking (Vector laboratories SP-2002) was conducted to prevent endogenous biotin binding. Sections were incubated in one of the following primary antibodies overnight at 4 ℃: rabbit polyclonal anti-Aβ1–42 (Abcam, ab12267, 1:300), rabbit recombinant anti-Aβ1–42 (mOC64, Abcam, ab201060, 1:800), rabbit recombinant anti-phospho-tau serine396 (S396, Abcam, ab109390, 1:6000), mouse monoclonal anti-phospho-tau serine202/threonine205 (AT8, Thermo-Fisher, MN1020, 1:100), or rabbit polyclonal anti-tau (DAKO #A0024, 1:10,000). Sections were incubated in 0.3% hydrogen peroxide for 10 minutes (RT) to prevent endogenous peroxide activity. Sections were incubated in the appropriate polyclonal biotinylated IgG goat anti-mouse or anti-rabbit secondary antibody (ThermoFisher Scientific, #62-6540, #65-6140, 1:300) with 1% w/v BSA for 1 hour (RT). Sections were incubated in streptavidin HRP (Abcam, ab64269) for 10 minutes (RT) and 3,3'-diaminobenzidine (DAB, Abcam, ab64238) for 5 minutes (RT), before being counterstained in haematoxylin. Negative control slides, omitting the primary antibody, and control slides where tissue was incubated directly in streptavidin and biotin, and DAB were prepared to determine the presence of any non-specific interactions.

2.5 Protein Extraction

Protein samples from the frontal cortex, entorhinal cortex and hippocampus were extracted from each of the stock sheep brains ($n = 30$) used in this study. Tissue was homogenised in 10 volumes of homogenisation buffer (TBS (50 mM Tris/HCl, pH 7.4) with 1 tablet of cOmplete™, Mini EDTA-free Protease Inhibitor Cocktail (Sigma-Aldrich®), and 1 tablet of PhosSTOP EASYpack (Sigma-Aldrich®) phosphate inhibitor. Homogenised tissue was centrifuged at 27,000 x *g* for one hour. The supernatant was collected as the soluble fraction and stored at -80°C until use.

2.6 Western Blot

Soluble protein sample concentrations were quantified using the Bradford Reagent assay. An aliquot (10 µg) of each sample was re-suspended in loading buffer (0.2 M Tris-HCl (pH 6.8), 8% w/v sodium dodecyl sulfate, 40% w/v glycerol, 0.02% bromophenol blue) with 50 mM Dithiothreeitol (DTT)) and boiled at 95°C for 10 minutes. Samples were separated on a 10% acrylamide gel using a mini-Protean (Biorad) kit, equilibrated with TGS gel running buffer (Biorad: 25 mM Tris, 192 mM glycine, 0.1% w/v SDS, pH 8.3). Proteins were transferred to a nitrocellulose membrane (0.45 µm pore size, Amersham™, Protran®). The membrane was blocked with 5% w/v skimmed milk in Tween 20 tris buffered saline (TTBS) overnight at 4°C. Membranes were incubated in mouse anti-human tau-46 monoclonal antibody (Thermo-Fisher, 1:1000), or recombinant rabbit anti-phospho-tau serine396 antibody (S396, Abcam, 1:10,000). The membrane was incubated in the appropriate IgG alkaline phosphatase conjugated secondary antibody (1:30,000) for 1 hour (RT). The membrane was developed for two minutes using the BCIP/NBT (5-Bromo-

4-chloro-3-indolyl phosphate/ nitro blue tetrazolium) system. Images were captured using a GS-800 calibrated densitometer (Biorad) and analysed with ImageQuant™ software.

2.7 Plasmid cloning PCR and sequence analysis

For the molecular analysis and isoform expression characterisation of tau, total RNA was extracted from the frontal cortex of one stock sheep (sheep #1) using a Direct-zol™ RNA Microprep Kit (Zymo Research). Complimentary DNA (cDNA) was created using the High Capacity RNA-to-cDNA™ Kit (Applied biosystems, Thermofisher Scientific). cDNA was used for subsequent PCR using three pairs of primers designed using the NCBI Predicted *Ovis aries* microtubule associated protein tau (MAPT) transcript, variant X1, XM_027974371.1 (Online Resource 1; table S1). PCR conditions consisted of 95°C for 3 minutes, followed by 45 cycles of 95°C for 30 seconds, 61°C for 1 minute, and 72°C for 2 minutes. A final extension of 30 minutes was used. PCR products were separated using a 2% agarose gel. Gels were visualised and analysed using a Typhoon FLA laser scanner (GE Healthcare). PCR products were excised from the gel and recovered using an ISOLATE II PCR and Gel Kit (Bioline). PCR products were ligated into a plasmid vector and transformed into Alpha-select bronze efficiency competent cells (Bioline) using the pGEM®-T Easy Vector system (Promega). Each transformation culture was plated onto ampicillin/IPTG/X-Gal LB-agar plates and incubated overnight at 37°C. Transformed colonies were picked and resuspended in 50 µl of nuclease free water. 10 µl was used for colony PCR and analysed using gel electrophoresis. Colonies with an appropriately sized insertion were cultured in 7 ml of LB broth (containing 100mg/ml ampicillin) overnight (37°C, 200 rpm). Plasmids were purified from the cell culture using an Isolate II Plasmid Mini Kit (Bioline) and underwent Sanger sequencing at the Translational Genomics Facility, Aberystwyth University. Multiple sequence alignments were performed using BioEdit Sequence Alignment Editor software [34]. Exons are described using standard exon nomenclature as detailed by Sündermann et al. [83].

2.8 Mass spectrometric analysis

Brain tissue samples (10µg) from four stock sheep > 5 years of age (sheep #1, 2, 3, 4) were separated by SDS-page electrophoresis using a 10% acrylamide gel. Five protein bands from each sample, which corresponded to the phospho-tau bands identified on western blot membranes were excised from the acrylamide gel. Briefly, gel pieces were de-stained in 50% v/v 50mM ammonium bicarbonate (pH 8) and 50% v/v acetonitrile (30 minutes at 37°C) until clear. Samples were dehydrated with 100% v/v acetonitrile (15 minutes at 37°C) and air dried (50°C). Samples were incubated with 100 µl, 10 mM DTT in ammonium bicarbonate (30 minutes 80°C). Samples were incubated with 55 mM IAA in ammonium bicarbonate (20 minutes, RT), and washed twice with 50% v/v ammonium bicarbonate and 50% v/v acetonitrile (15 minutes, RT). Samples were dehydrated, air dried, and rehydrated in 50 mM ammonium bicarbonate containing 10 ng/µl trypsin (modified trypsin sequencing grade, Promega), overnight at 37°C. Samples were eluted in 20–50 µl of water, followed by 50% v/v acetonitrile, with 5% v/v formic acid. Elutant was dried and stored at -20°C. Samples were re-constituted using 20 µl 0.1% v/v formic acid immediately before analysis.

Liquid chromatography mass spectrometry was conducted using an Orbitrap Fusion™ Tribrid™ mass spectrometer (Thermo Scientific™), with H-ESI ion source, coupled to an UltiMate™ 3000 UHPLC tower (Dionex, Thermo Scientific ™) comprised of a rapid separation pump, column compartment and auto-sampler. Liquid chromatography was conducted with an Agilent eclipse plus C18 column (2.1 x 5 mm, with 1.8 μM particle size). The mobile phases for gradient elution were ultrapure water (18.2Ω) with 0.1% formic acid as elutant 1, and 95% aceronitrile with 0.1% formic acid as elutant 2. Liquid chromatography was performed with a flow rate of 0.1 ml/min starting with elutant 2 at 3–40% for 9 minutes, 40–100% for 2 minutes, and 100% for 1 minute, before equilibration at 3% for 1.5 minutes. Ions were generated in a H-ESI source with a source voltage of 3500 V in positive mode, sheath gas: 25, aux gas: 5, a vaporiser temperature of 75°C and an ion transfer temperature of 275°C. Standard peptide analysis parameters were used; parent ions were detected in profile mode in the 375–1500 m/z range in the orbitrap at a resolution of 120,000 and a maximum injection time of 50 ms in positive mode. MS2 data was collected in data dependent mode including charge states of 2–7. Dynamic exclusion of masses was conducted for 20 seconds after initial selection for MS2. Ions were formed by fragmentation by collision induced dissociation with a collision energy of 35%. Resulting ions were detected in the Ion Trap in centroid mode.

Mass spectral data was submitted to the MASCOT (www.matrixofscience.com) for database comparison. Spectre were searched against the Ensembl *Ovis Aries* (Oar_v3.1) protein database. Search parameters allowed up to one missed cleavage and included a fixed peptide modification of carbamidomethylation and a variable modification of oxidised methionine residues. Peptide charges 2+, 3 + and 4 + were selected for analysis. Parameters also included a set peptide tolerance of ± 1.2 Da and a MS/MS tolerance of ± 0.6 Da. Individual sequences were compared against a transcript protein map generated using the NCBI Predicted *Ovis aries* MAPT transcript, variant X1, XM_027974371.1, and the NCBI sequence, XP_027830172.1 using exon nomenclature described by Sündermann et al. [83].

2.9 Statistical analysis

Twenty of the brains (from stock animals 1–2 and > 5 years of age) were examined using immunohistochemistry. The number of positive regions labelled using the AT8 antibody were verified via microscopy and manually counted. Samples from all brains in the main study were used for western blot analysis. The relative intensities of the positive signals, probed with the anti-phospho-tau antibody, S396, were quantified using ImageQuant™ software. The average signal intensities were measured, standardised, and the background signal was controlled for using the local median value. As on balance, both of these data (average number of AT8 positive regions identified and western blot signal intensity) met the assumptions for parametric statistical analysis, the effect of age, brain region and the interaction of these two factors on the data were analysed using a two-way analysis of variance (ANOVA), with Tukey HSD post hoc testing. Data are reported as mean ± S.E.M.

3.0 Results

3.1 Pilot Study

Immunohistochemistry using the anti-phospho-tau antibody AT8 identified numerous mature NFTs throughout the neocortex of the 21 year-old sheep (P1). The NFTs were particularly concentrated within layer III of the insular cortex and olfactory tract (Fig. 1). Immunohistochemistry using the anti-Aβ1–42 antibody, ab12267, identified numerous diffuse Aβ plaques in the parietal cortex of the 16 year-old sheep (P2) (Fig. 2; A). No dense-cored plaques were detected.

Figure 1 near here

3.2 β-amyloid immunohistochemistry

3.2.1 Neuronal tissue

Immunohistochemistry using the anti-Aβ1–42 antibody, ab12267, detected a very small number of immuno-positive regions, identified as diffuse Aβ deposits in the entorhinal and temporal cortex of one individual > 5 years of age (sheep #5; Table 1 & Fig. 2; B). No diffuse Aβ deposits were detected in 1–2 year-old sheep, and no dense-cored plaques were detected in any of the brains examined. However, this antibody labelled the cytoplasm of large neurons in the pons of all 1–2 and > 5 year-old sheep (for example Fig. 2; C & D).

Table 1
Immunohistochemical detection of Aβ and phosphorylated tau in 1–2 and > 5 year old sheep.

Age range (animal identifier)	Diffuse Aβ plaques (ab12267)	Vascular Aβ labelling (ab12267)	Vascular Aβ labelling (mOC64)	Hippocampal CA3 region (mOC64)	Hippocampal CA3 region (S396)	Pre-tangles (AT8)
> 5 (1–10)	+ (5)	+ (2, 5, 7, 8, 9, 10)	++ all	++ all	+ (2, 3, 9) ++ (1, 4, 5, 6, 7, 8, 10)	+ (1, 4, 6)
1–2 (11–20)	-	+ (11, 12, 18)	+ (13, 16, 17, 18, 20) ++ (11, 12, 14, 15,19)	+ (11, 13, 14, 15, 16, 17, 18, 19)	+ (12, 14, 15, 17, 19) ++ (11, 13, 16, 18, 19)	-

+; partial immunopositivity (observed in a small number of cells), ++; abundant immunopositivity, -; no immunopositive labelling, brackets indicate in which individual animal (1–10; animals > 5 years old, 11–20; animals 1–2 years old) immunopositivity was identified.

Immunohistochemistry using the anti-Aβ1–42 antibody, mOC64, positively labelled neurons in layers II, III and V of the hippocampal, entorhinal and parietal cortices of all individuals > 5 years of age (for example Fig. 3; A & B). The cell bodies of the stratum pyramidale and neuronal processes of the substratum radiatum within the CA3 region of the hippocampus were also clearly labelled in all sheep > 5 years old (for example Fig. 6; C). These structures within the hippocampus were also partially or faintly labelled in 8 out of 10 1–2 year-old sheep (for details of individual sheep see Table 1).

Human AD brain samples were used as positive control tissue. Both the anti-Aβ1–42 antibodies, ab12267 and mOC64 labelled Aβ plaques with minimal background signal present (Online Resource 2; figure S1).

3.2.2 Vascular Tissue

Many small arterial and capillary walls within the pons of both 1–2 and > 5 year-old sheep were positively labelled using the ab12267 antibody (for example Fig. 4). Immunopositivity was not always confined to vessel walls, and often extended into the vessel lumen. Arterial and capillary walls within the hippocampus, entorhinal cortex, parietal cortex and pons of 1–2 and > 5 year-old sheep were also labelled using the mOC64 antibody. Vascular labelling with this antibody was confined to the vessel walls and appeared primarily within the tunica media.

Table 1, **Fig. 2, Fig. 3, Fig. 4 near here**

3.3 Tau immunohistochemistry

Immunohistochemistry using the anti-phospho-tau antibody, AT8, labelled three structures identified as pre-neurofibrillary tangles within the entorhinal cortex of three sheep > 5 years of age (sheep #1, #4 and #6) (Fig. 5). No mature NFTs were identified using the AT8 antibody in any of the brain regions of 1–2 year-old or > 5 year-old sheep.

Immunohistochemistry using the anti-phospho-tau antibody, S396, resulted in a very distinct and defined pattern of immunopositivity that was limited to the neuronal processes of the substratum radiatum of the CA3 region of the hippocampus (Fig. 6; A). By contrast to the mOC64 antibody (Fig. 6; C), however, no labelling of the cell bodies occurred with the use of the S396 antibody. This pattern of staining was clearly demonstrated in 7 out of 10 sheep aged > 5 years, and 5 out of 10 sheep aged 1–2 years. The remaining sheep exhibited partial labelling of this region that was restricted to only a few neurites (Table 1).

Immunohistochemistry using the pan-tau antibody, DAKO-0024, also resulted in the positive labelling of neuronal processes of the substratum radiatum of the CA3 region. However, as with the use of the mOC64 antibody, the use of the DAKO-0024 antibody also positively labelled the soma of neurons within this region (Fig. 6; B).

Both the anti-phospho-tau antibodies, AT8 and S396, labelled NFTs in human AD tissue, used as a positive control, with minimal background signal present (Online Resource 2; figure S1).

Figure 5, Fig. 6 near here

3.4 Atypical AT8 labelling

Immunohistochemistry using the anti-phospho-tau antibody, AT8, resulted in a number of diffuse plaque-like immuno-positive regions throughout the parietal cortex and pons of both 1–2 and > 5 year-old sheep. The hippocampus and entorhinal cortex of sheep > 5 years old also exhibited small numbers of these diffuse plaque-like positive areas, though none were identified within the same brain regions of 1–2 year-

old sheep. These positively labelled areas did not show a morphology characteristic of tau pathology such as neuropil threads or NFTs. Rather they appeared as discrete amorphic structures, more closely resembling diffuse Aβ deposits. These ranged in appearance from small diffuse regions the size of single cells, to very dense large areas, many times larger than a single cell (Fig. 7). However, these regions were not positively labelled using Aβ antibodies, and the areas of AT8 labelling did not resemble tau pathology that would normally accompany dense-cored plaques. Given that all control slides were devoid of any staining, non-specific interactions (e.g. resulting from tissue artefacts, secondary antibody labelling, or endogenous biotin and peroxidase labelling) were ruled out. A two-way ANOVA was undertaken to test the effect of age, brain region and also the interaction between age and brain region on the quantity of AT8 positive areas identified. Results showed that there was a significant interaction between age and brain region on the number of AT8 positive regions identified (F (2,54) = 22.04, $p < 0.001$). Tukey HSD post-hoc tests were conducted. For sheep > 5 years of age, the number of positive AT8 areas identified in the parietal cortex was significantly greater than in the pons ($p < 0.001$) and hippocampus ($p < 0.001$). The number of AT8 positive regions identified in the pons was also significantly greater than in the hippocampus ($p = 0.001$). For sheep 1–2 years of age the number of positive AT8 areas identified in the parietal cortex was significantly greater than in the hippocampus ($p = 0.02$). No significant differences in the number of AT8 positive areas between the parietal cortex and pons, or pons and hippocampus were detected. Additionally, the number of AT8 positive regions identified in the parietal cortex and pons of sheep > 5 years of age was significantly greater than for sheep 1–2 years of age ($p < 0.001$ and $p = 0.042$ respectively). No significant difference for the hippocampus between age groups was identified. Therefore, although the number of AT8 positive areas identified was greater for sheep that are > 5 years of age, compared to sheep that are 1–2 years of age, the difference in the number of areas identified between these two groups varied between brain regions (Fig. 8).

Figure 7 and Fig. 8 near here

3.5 Expression of tau isoforms

To confirm the splice variants of ovine tau, tau transcripts from one sheep (sheep #1) were examined using plasmid PCR cloning. Samples from four sheep (sheep # 1, 2, 3, 4) were also analysed using mass spectrometry. Primer pair 1 which spanned exons 1–14 resulted in the amplification of multiple cDNA products between approximately 800 and 1300 base pairs in length. Following the successful ligation of these products into the plasmid vector, and subsequent transformation into competent cells, 15 complete tau cDNA clone products were sequenced. Sequence analysis showed that while exon 3 was present in all transcripts, alternative splicing of exons 4 and 12 occurred, resulting in the expression of four distinct tau isoforms, identified as 2N4R (+ 3, 4, 12), 2N3R (+ 3, 4), 1N4R (+ 3, 12) and 1N3R (+ 3) tau isoforms (Fig. 9). The splicing of exons 4 and 12 was confirmed using primer pairs 2 and 3. Primer pair 2 which spans exons 1–7 resulted in the amplification of two distinct cDNA bands, between approximately 300 and 500 base pairs in length. The sequencing of these bands confirmed the splicing of exon 4. Primer pair 3, which spans exons 7–15 resulted in the amplification of two distinct cDNA bands, between approximately 800 and 1100 base pairs in length. The sequencing of these bands confirmed the splicing

of exon 12. No indication for the splicing of exon 3, which occurs in humans was observed following PCR, plasmid cloning or transcript sequencing. Exons 6, 8 and 10 are not transcribed in human tau, and similarly, this study found no evidence to suggest the transcription of these exons in ovine tau. An NCBI BLAST alignment demonstrated that the transcribed coding regions, from exon 2 to exon 15, of the experimental tau transcripts generated in this study shared 99.9% identity with the same regions of the longest predicted reference ovine tau transcript, XM_027974371.1. One nucleotide substitution, identified within exon 11, resulted in the replacement of a cytosine included in the reference transcript with a thymine, resulting in a synonymous substitution. As a result, the longest ovine tau protein, consisting of 432 amino acids, confirmed in this study, shares 90.52% homology with the longest human CNS tau isoform (NCBI, NP_005901.2), and 90.07% homology with the longest murine CNS tau isoform (NCBI, NP_001033698.1) (Online Resource 3; figure S2). Mass spectrometric analysis identified peptides translated from each of the exons identified during the PCR cloning of cDNA, providing further evidence for the existence of four MAPT splice variants in the adult ovine cerebral cortex (Online Resource 1; table S2). A comparison of the tau variants expressed in the adult brains of a range of species is included in Fig. 10.

Figure 9, Fig. 10 near here

3.6 Phosphorylation of tau serine396

Tau phosphorylation at residue serine396 was examined using western blotting. Tau phosphorylated at this epitope was detected in soluble samples from the hippocampus, entorhinal cortex and frontal cortex of all ten sheep > 5 years of age. Tau phosphorylated at residue serine396 was also detected in the hippocampus, entorhinal cortex and frontal cortex of 7 out of 10 sheep 2–3 years of age. Additionally, tau phosphorylated at serine396 was detected in samples from the hippocampus, entorhinal cortex and frontal cortex of two out of ten 1–2 year-old sheep (sheep #16 & #17). When the relative intensities of the western blots were compared (Fig. 11), there was no statistically significant difference in mean intensity between brain regions ($F(2,81) = 0.259$, $p = 0.772$), but there were statistically significant differences between age groups ($F(2,81) = 18.26$, $p < 0.001$). There was no statistically significant interaction of these two factors on mean intensity ($F(4,81) = 0.129$, $p = 0.971$). Post-hoc analysis indicated that signal intensity of tau abundance in sheep > 5 years of age was statistically significantly greater than the signal intensity of sheep 1–2 years of age ($p < 0.001$). The signal intensity of sheep 2–3 years of age was also statistically significantly greater than sheep aged 1–2 years old ($p < 0.001$). However, there were no statistically significant differences in signal intensity when sheep 2–3 and > 5 years old were compared directly ($p = 0.195$).

Figure 11 near here

4.0 Discussion

4.1 Aβ pathology

Previous studies have reported that both Aβ and tau pathology occurs naturally in sheep brain [60, 67]. Our pilot study using two very old sheep identified numerous mature NFTs and diffuse Aβ deposits. We extended these findings by characterising AD-like Aβ and tau pathology in sheep sourced from the commercial sheep population. We detected a small number of diffuse Aβ deposits in the entorhinal cortex of only one individual aged > 5 years but found intraneuronal Aβ-42 labelling using the mOC64 antibody in all sheep > 5 years of age. The presence of intraneuronal oligomeric Aβ species is considered an early aetiological event that precedes extracellular plaque and NFT formation and has been described extensively in humans with AD [18, 31, 32, 55, 65, 84, 90], and in transgenic mouse models of AD [49, 63, 64]. Intraneuronal oligomeric Aβ has also been described in cases of spontaneous AD-like pathology in cats [12], dogs [16] and dolphins [81]. Our data support earlier findings of AD-like pathology in sheep. Our data support earlier findings of AD-like pathology in sheep [60, 67].

Vascular Aβ deposition was detected throughout the brains of 1–2 and > 5 year-old sheep. The presence of vascular Aβ labelling in the absence of parenchymal Aβ deposition is particularly interesting as it has been hypothesised that both red blood cell and cerebral vascular damage may be key processes that contribute to the development of Aβ plaques [50, 76]. It is not clear whether these processes lead to increased parenchymal Aβ deposition due to cellular hypometabolism or increase the influx of Aβ enriched proteins from blood derived cells. However, it has been suggested that CAA may represent an intermediate stage in the process of Aβ plaque formation [24, 39, 50, 82].

Aβ deposition and NFTs have previously been identified in eight-year-old sheep using the monoclonal mouse antibody, clone 4G8 [67]. Those Aβ deposits were described as large dense structures, occurring throughout all cortical regions, including the hippocampus. Numerous small areas of staining, the size of a single neuronal nuclei, were also described. Aβ deposits consistent with those described by Reid et al. [67] were not identified in this study. The absence of large Aβ deposits may be due to the younger age of the sheep we examined. The absence of small deposits, however, is more likely to reflect the use of a different antibody. Reid et al [67] used the clone 4G8, that recognises the Aβ epitope between amino acids 18 and 22 and is unable to distinguish Aβ from APP and other Aβ-containing APP fragments [2, 32]. As a result, the amount of Aβ deposition reported previously may have been overestimated.

4.2 Tau pathology and phosphorylation

In the current study, while no mature NFTs were detected, three AT8 positive pre-neurofibrillary tangles [5] were identified in sheep > 5 years of age. In humans, the differential phosphorylation of tau residues occurs in a temporal pattern correlated with disease progression [86]. Phosphorylation of residue serine396 is generally considered to be an early pathological event, associated with tau oligomerization [29, 51, 56, 66, 89]. Thus, the S396 antibody is commonly used to study early tau hyperphosphorylation in a range of species and AD models [1, 27]. In contrast, the phosphorylation of residues serine202 and threonine205, detected by the AT8 antibody, occurs in the latter stages of tau pathology [30]. Although it is likely that the absence of mature NFTs reflects the relatively young age of the sheep included in this study, the presence of pre-neurofibrillary tangles are indicative of early-stage tau pathology being present in sheep as young as 5–8 years of age [67]. As the preliminary study of a 21 year-old sheep detected

numerous AT8 positive mature NFTs, it is likely that sheep of significant age have the potential to reflect the advanced stage tau pathology observed in AD, and that early stage tau pathology observed in younger sheep may eventually progress to this advanced stage. Together these findings support the results of previous studies which identified NFTs phosphorylated at the AT8 epitope [7, 61].

Phosphorylation of the serine396 residue was also investigated. We found phosphorylated S396 immunoreactivity was present in some sheep 2 years of age and that phosphorylation increased with age. While the observation of this pathology at such an early age may be surprising, it is consistent with human data where it has been shown that abnormal tau changes occur in the brain as early as childhood or puberty [8, 9]. Recent evidence also suggests that neurons undergo a dying back pattern of degeneration, where tau pathology begins in the axonal compartment before progressing to the somatodendritic compartment [14, 48]. The differential patterns of immunostaining within the CA3 region of the hippocampus observed using different anti-Aβ-42 and anti-tau antibodies in this study may indicate early hippocampal intraneuronal Aβ deposition, accompanied by early-stage axonal tau phosphorylation. The presence of mOC64 and S396 immunopositivity may also indicate that these changes occur in sheep as young as approximately 2 years of age. The pattern of S396 labelling within the CA3 region of the hippocampus is remarkably similar to labelling detected using the same antibody in the hippocampus of cows with idiopathic brainstem neuronal chromatolysis (IBNC) [45]. While the exact aetiological cause of IBNC is unknown, studies have indicated that it is a complex proteinopathy characterised by significant hyperphosphorylated tau with associated secondary accumulations of alpha-synuclein and ubiquitin, without associated NFT formation or amyloid deposition [45]. Interestingly, while cases of IBNC are predominantly reported in cows > 6 years old, the youngest recorded case was in a cow just four years old. Therefore, further research into tau phosphorylation and tauopathy in sheep and large ruminants would be beneficial, to determine if these two pathologies are related.

The current study identified diffuse plaque-like tau positive regions that were not characteristic of AD-like tau pathology. These may have resulted from non-specific antibody staining, however, the use of the AT8 antibody is renowned for achieving specific phospho-tau labelling with little or no background signal [7, 30]. We found no background staining in the tissue surrounding these focal regions. All control slides were also negative, and the pattern of staining with the AT8 antibody on both AD positive and AD negative human control tissue was as expected, with staining only of the AD patient brain. Given that the regional and age-dependent distribution of these AT8 positive elements is consistent with a progressive pathogenesis, it is likely that the AT8 antibody in this instance is accurately labelling phosphorylated tau. Further investigations into possible sources of this atypical AT8 labelling in sheep are necessary.

4.3 Tau isoform expression

In humans, all six of the tau isoforms expressed in the brain become hyper-phosphorylated and involved in tau pathology. MAPT splicing and tau isoform expression, however, differs between species, affecting the subsequent formation of tau pathology [37, 77, 85]. This study confirmed the expression of the four distinct ovine tau isoforms described by Janke et al. [44], formed from the splicing of exons 4 and 12. This pattern of ovine tau expression is consistent with the phylogenetic expression of tau in other

ruminants [40, 44]. While exon 10 has previously been identified in transcripts from the rhesus macaque and the cow [62] the ovine tau transcripts generated in this study confirmed that exons 6, 8 and 10 are not transcribed in sheep (for comparisons of tau expression between species, see Fig. 10). Janke *et al*. [44] also described two additional isoforms in sheep, interpreted as the two 0N tau isoforms, consistent with the two shortest tau isoforms expressed in humans. However, we found no evidence for the expression of these isoforms, resulting from the alternative splicing of exon 3. The confirmation that sheep express the 3R and 4R tau isoforms that are expressed in humans is an important step in assessing of their suitability as an AD model, particularly given that mice naturally express only 4R tau [3]. Possessing both 3R and 4R endogenous tau isoforms confers considerable potential to the sheep as an AD model with a highly translatable value.

The variations in the tau N-terminal projection domains of different species have been cited as reasons why tau pathology differs between species [3]. The human N-terminal domain contains an eleven amino acid motif (residues 17–28) not present within the N-terminal domain of murine tau [37]. This additional peptide sequence is thought to affect the intramolecular interactions between the N- and C-terminals, and the microtubule-binding domains of tau, increasing the likelihood of normal tau undergoing pathological conformational changes [3, 37]. The lack of this N eleven amino acid motif in murine tau has been suggested as one reason why mice do not naturally develop any tau pathology [37]. Additionally, within the first 190 N-terminal amino acids, human tau contains 33 serine, threonine, and tyrosine residues. Murine tau shares 22 of these residues. Many of the residues, found in humans (but lacking in mice) are phosphorylated in AD, or are phosphorylated by kinases that exhibit dysregulation in AD [35]. However, an alignment of the human, murine and ovine tau proteins show that sheep lack the eleven amino acid sequence, and many of the same phosphorylation sites as murine tau, even though they naturally develop tau pathology [7, 60, 61, 67]. We speculate that while the presence of the 11 amino acid motif and the phosphorylation of these residues may accelerate pathological tau formation in humans, their involvement is not essential for the development of PHF tau.

Proline rich regions facilitate the phosphorylation of serine and threonine residues via kinases thought to have key roles in the pathogenesis of AD [41]. There are seven distinct variations between the human and ovine proline rich regions of tau that may be implicated in tau hyperphosphorylation in the sheep. For example, proline176, alanine178 and proline182 in human tau are substituted with threonine, threonine and serine respectively in ovine tau. However, proline residues that are important for the directed phosphorylation of tyrosine residues such as proline213, proline216 and proline219 are conserved between humans and sheep [37, 52]. Additionally, each of the four KXGS motifs which can be phosphorylated by multiple kinases, and the four PGGG sequences which facilitate the formation of type II β-turns and β-hairpin structures, are conserved between humans and sheep [13, 20].

4.4 Future Work

As only three other studies have used phosphorylation dependent antibodies on ovine brain tissue further work is required to elucidate the residue specific patterns of tau phosphorylation in sheep as they age. This study focused on the hippocampus and entorhinal cortex. Although these are considered to be

critical regions for the development of AD pathology, future studies would benefit from analysing adjacent subcortical structures that have been implicated in the early tau pathology of both humans and aged canines, such as the thalamus [1]. A complete evaluation of other protein pathologies, such as those involving ubiquitin, APOE and GFAP would also be beneficial since this would provide a more complete picture of AD-related pathology in sheep [53]. Environmental factors that could increase the likelihood of sheep developing AD-like pathologies also need to be investigated. For example, both copper (to which sheep are sensitive), and rumen-protected feed ingredients such as formaldehyde are factors that have been implicated in AD pathogenesis [45, 80, 91]. They may contribute to the AD-like pathology observed in other young ruminants. Future studies will also benefit from a complete evaluation of potential heterozygous substitutions and single nucleotide polymorphisms of the ovine MAPT transcript. Finally, screening sheep for relevant alleles, such as APOEε4 may help to enhance the detection of AD-like pathological characteristics in the commercial sheep population, increasing their potential suitability of being a natural AD model [67, 87].

5.0 Conclusion

We identified intracellular and vascular Aβ deposition in the brains of sheep as young as two years of age. We also identified AT8 positive pre-neurofibrillary tangles in sheep > 5 years of age. One of the early stages in the conversion of normal to pathological tau is the phosphorylation of multiple residues. We show that even by two years of age, some phosphorylation of the serine396 residue is present in sheep, and the relative amount of tau phosphorylated at this residue increases with advancing age. Given that these findings are consistent with early-stage AD-like pathology, sheep could be used to investigate the early biochemical and structural changes that eventually result in advanced AD-like pathology, without the complications of late-stage pathology. This would be an important step, given that the disease course of rodent transgenic AD models often progresses too rapidly for a comprehensive evaluation of this pre-clinical phase of AD aetiology to be completed [22]. Our pilot study detected numerous NFTs in a sheep 21 years of age, indicating that the development of late-stage tau pathology is possible in older sheep. This study has also confirmed that sheep express four distinct tau isoforms in their CNS, composed of three and four binding repeats, which result from the alternative splicing of exons 4 and 12. As a result, the sheep, as either a spontaneous model, perhaps with genetic predisposition, or a transgenic model, has the potential to provide a valuable model of early-stage AD-like tauopathy, reflective of that seen in humans.

Abbreviations

AD: Alzheimer’s Disease; Aβ: β-amyloid; CAA: Cerebral amyloid angiopathy; NFTs: Neurofibrillary tangles; APP: Amyloid precursor protein; PSEN1: Presenilin 1; PSEN: Presenilin 2; FTDP-17; Frontotemporal dementia with parkinsonism-17; FAD: Familial Alzhimer’s Disease; TBS: Tris-buffered saline; RT: room temperature; DTT: Dithiothreeitol; TTBS: Tween 20 tris buffered saline; BCIP/NBT: 5-Bromo-4-chloro-3-indolyl phosphate/ nitro blue tetrazolium; IPTG: Isopropyl β- d-1-thiogalactopyranoside; X-GAL: 5-Bromo-

4-Chloro-3-Indolyl β-D-Galactopyranoside; LB: Luria-Bertani; IBNC: Idiopathic brainstem neuronal chromatolysis; CNS: central nervous system; MAPT: Microtubule associated protein tau; PCR: polymerase chain reaction; ANOVA: Analysis of variance; CA3: Cornu ammonis 3; NCBI: National Centre for Biotechnology Information; PHFs: Paired helical filaments; APOE: Apolipoprotein; GFAP: Glial fibrillary acidic protein.

Declarations

Ethical approval: This study was conducted in accordance with the Scientific Procedures Act 1986 and the study received ethics approval and consent granted by Aberystwyth University's Animal Welfare Ethical Review Body.

Data availability: Supplementary information accompanies this paper. Datasets analysed and presented in the current study are available from the corresponding author on request.

Competing Interests: Authors have no competing interests.

Author Contributions: ED, AJM, RM and SMcB designed the study experiments, ED conducted the experiments, analysed the results, and wrote the manuscript. RM provided research equipment and technical expertise. DC provided technical expertise. SMcB, RM, DC and AJM critically revised the manuscript.

Funding: This research was funded by NRN Life Sciences Research Network Wales.

Acknowledgements: The authors would like to acknowledge the technical assistance and support relating to brain sample collection provided by Naomi Gordon. We thank Mrs Kath Bretnall for the gift of the aged pilot sheep brains and Mrs Wendy Leavens and Zhiguang Zheng for histology and technical assistance relating to the pilot sheep data. We would also like to acknowledge the support received from the Translational Genomics Facility of Aberystwyth University

References

1. Abey A, Davies D, Goldsbury C, Buckland M, Valenzuela M, Duncan T (2021) Distribution of tau hyperphosphorylation in canine dementia resembles early Alzheimer's disease and other tauopathies. Brain Pathol 31(1):144–162
2. Aho L, Pikkarainen M, Hiltunen M, Leinonen V, Alafuzoff I (2010) Immunohistochemical visualization of amyloid-β protein precursor and amyloid-β in extra-and intracellular compartments in the human brain. J Alzheimers Dis 20(4):1015–1028
3. Ando K, Leroy K, Héraud C, Yilmaz Z, Authelet M, Suain V, De Decker R, Brion JP (2011) Accelerated human mutant tau aggregation by knocking out murine tau in a transgenic mouse model. Am J Pathol 178(2):803–816

4. Arnsten AF, Datta D, Leslie S, Yang ST, Wang M, Nairn AC (2019) Alzheimer's-like pathology in aging rhesus macaques: Unique opportunity to study the etiology and treatment of Alzheimer's disease. *Proceedings of the National Academy of Sciences*, *116*(52), pp.26230–26238
5. Augustinack JC, Schneider A, Mandelkow EM, Hyman BT (2002) Specific tau phosphorylation sites correlate with severity of neuronal cytopathology in Alzheimer's disease. Acta Neuropathol 103(1):26–35
6. Bond M, kleine Holthaus SM, Tammen I, Tear G, Russell C (2013) Use of model organisms for the study of neuronal ceroid lipofuscinosis. Biochim et Biophys Acta (BBA)-Molecular Basis Disease 1832(11):1842–1865
7. Braak H, Braak E, Strothjohann M (1994) Abnormally phosphorylated tau protein related to the formation of neurofibrillary tangles and neuropil threads in the cerebral cortex of sheep and goat. Neurosci Lett 171(1–2):1–4
8. Braak H, Del Tredici K (2011) The pathological process underlying Alzheimer's disease in individuals under thirty. Acta Neuropathol 121(2):171–181
9. Braak H, Del Tredici K (2012) Where, when, and in what form does sporadic Alzheimer's disease begin? Curr Opin Neurol 25(6):708–714
10. Buée L, Bussière T, Buée-Scherrer V, Delacourte A, Hof PR (2000) Tau protein isoforms, phosphorylation and role in neurodegenerative disorders. Brain Res Rev 33(1):95–130
11. Calderon-Garcidueñas AL, Duyckaerts C (2018) Alzheimer disease. Handbook of Clinical Neurology, vol 145. Elsevier, pp 325–337
12. Chambers JK, Tokuda T, Uchida K, Ishii R, Tatebe H, Takahashi E, Tomiyama T, Une Y, Nakayama H (2015) The domestic cat as a natural animal model of Alzheimer's disease. *Acta Neuropathologica Communications*, *3*(1), p.78
13. Chen D, Drombosky KW, Hou Z, Sari L, Kashmer OM, Ryder BD, Perez VA, Woodard DR, Lin MM, Diamond MI, Joachimiak LA (2019) Tau local structure shields an amyloid-forming motif and controls aggregation propensity. *Nature Communications*, *10*(1), pp.1–14
14. Christensen KR, Beach TG, Serrano GE, Kanaan NM (2019) Pathogenic tau modifications occur in axons before the somatodendritic compartment in mossy fiber and Schaffer collateral pathways. Acta Neuropathol Commun 7(1):1–21
15. Cocquyt G, Driessen B, Simoens P (2005) Variability in the eruption of the permanent incisor teeth in sheep. Vet Rec 157(20):619–623
16. Cummings BJ, Su JH, Cotman CW, White R, Russell MJ (1993) β-amyloid accumulation in aged canine brain: a model of early plaque formation in Alzheimer's disease. Neurobiol Aging 14(6):547–560
17. Cummings BJ, Head E, Afagh AJ, Milgram NW, Cotman CW (1996) β-amyloid accumulation correlates with cognitive dysfunction in the aged canine. Neurobiol Learn Mem 66(1):11–23
18. D'Andrea MR, Nagele RG, Wang HY, Peterson PA, Lee DH (2001) Evidence that neurones accumulating amyloid can undergo lysis to form amyloid plaques in Alzheimer's disease.

Histopathology 38:120–134

19. DeTure MA, Dickson DW (2019) The neuropathological diagnosis of Alzheimer's disease. Mol Neurodegeneration 14(1):1–18
20. Dehmelt L, Halpain S (2004) The MAP2/Tau family of microtubule-associated proteins. *Genome Biology*, *6*(1), p.204
21. Drummond E, Wisniewski T (2017) Alzheimer's disease: experimental models and reality. Acta Neuropathol 133(2):155–175
22. Eaton SL, Wishart TM (2017) Bridging the gap: large animal models in neurodegenerative research. Mamm Genome 28(7–8):324–337
23. Eaton SL, Proudfoot C, Lillico SG, Skehel P, Kline RA, Hamer K, Rzechorzek NM, Clutton E, Gregson R, King T, O'Neill CA (2019) CRISPR/Cas9 mediated generation of an ovine model for infantile neuronal ceroid lipofuscinosis (CLN1 disease). Sci Rep 9(1):1–8
24. Edler MK, Sherwood CC, Meindl RS, Hopkins WD, Ely JJ, Erwin JM, Mufson EJ, Hof PR, Raghanti MA (2017) Aged chimpanzees exhibit pathologic hallmarks of Alzheimer's disease. Neurobiol Aging 59:107–120
25. Elder GA, Gama Sosa MA, De Gasperi R (2010) Transgenic mouse models of Alzheimer's disease. Mt Sinai J Medicine: J Translational Personalized Med 77(1):69–81
26. Flattery CNR, Rosen RF, Farberg AS, Dooyema JM, Hof PR, Sherwood CC, Walker LC, Preuss TM (2020) Quantification of neurons in the hippocampal formation of chimpanzees: comparison to rhesus monkeys and humans. Brain Struct Function 225(8):2521–2531
27. Foidl BM, Humpel C (2018) Differential hyperphosphorylation of tau-S199,-T231 and-S396 in organotypic brain slices of Alzheimer mice. A model to study early tau hyperphosphorylation using okadaic acid. *Frontiers in Aging Neuroscience*, *10*, p.113
28. Gearing M, Rebeck GW, Hyman BT, Tigges J, Mirra SS (1994) Neuropathology and apolipoprotein E profile of aged chimpanzees: implications for Alzheimer disease. *Proceedings of the National Academy of Sciences*, *91*(20), pp.9382–9386
29. Goedert M, Jakes R, Crowther RA, Cohen P, Vanmechelen E, Vandermeeren M, Cras P (1994) Epitope mapping of monoclonal antibodies to the paired helical filaments of Alzheimer's disease: identification of phosphorylation sites in tau protein. Biochem J 301(3):871–877
30. Goedert M, Jakes R, Vanmechelen E (1995) Monoclonal antibody AT8 recognises tau protein phosphorylated at both serine 202 and threonine 205. Neurosci Lett 189(3):167–170
31. Gouras GK, Tsai J, Naslund J et al (2000) Intraneuronal Abeta42 accumulation in human brain. Am J Pathol 156:15–20
32. Gouras GK, Tampellini D, Takahashi RH, Capetillo-Zarate E (2010) Intraneuronal β-amyloid accumulation and synapse pathology in Alzheimer's disease. Acta Neuropathol 119(5):523–541
33. Geula C, Nagykery N, Wu CK (2002) Amyloid-β deposits in the cerebral cortex of the aged common marmoset (Callithrix jacchus): incidence and chemical composition. Acta Neuropathol 103(1):48–58

34. Hall TA (1999) BioEdit: a user-friendly biological sequence alignment editor and analysis program for Windows 95/98/NT. 41:95–98
35. Hanger DP, Byers HL, Wray S, Leung KY, Saxton MJ, Seereeram A, Reynolds CH, Ward MA, Anderton BH (2007) Novel phosphorylation sites in tau from Alzheimer brain support a role for casein kinase 1 in disease pathogenesis. J Biol Chem 282(32):23645–23654
36. Hardy J, Allsop D (1991) Amyloid deposition as the central event in the aetiology of Alzheimer's disease. Trends Pharmacol Sci 12:383–388
37. Hernández F, Merchán-Rubira J, Vallés-Saiz L, Rodríguez-Matellán A, Avila J (2020) Differences between human and murine Tau at the N-terminal end. *Frontiers in Aging Neuroscience*, *12*, p.11
38. Heuer E, Rosen F, Cintron R, Walker C, L (2012) Nonhuman primate models of Alzheimer-like cerebral proteopathy. Curr Pharm Design 18(8):1159–1169
39. Hohsfield LA, Humpel C (2015) Migration of blood cells to β-amyloid plaques in Alzheimer's disease. Exp Gerontol 65:8–15
40. Himmler A (1989) Structure of the bovine tau gene: alternatively spliced transcripts generate a protein family. Mol Cell Biol 9(4):1389–1396
41. Hooper C, Killick R, Lovestone S (2008) The GSK3 hypothesis of Alzheimer's disease. J Neurochem 104(6):1433–1439
42. Hough D, Bellingham M, Haraldsen IRH, McLaughlin M, Rennie M, Robinson JE, Solbakk AK, Evans NP (2017) Spatial memory is impaired by peripubertal GnRH agonist treatment and testosterone replacement in sheep. Psychoneuroendocrinology 75:173–182
43. Jacobsen JC, Bawden CS, Rudiger SR, McLaughlan CJ, Reid SJ, Waldvogel HJ, MacDonald ME, Gusella JF, Walker SK, Kelly JM, Webb GC (2010) An ovine transgenic Huntington's disease model. Hum Mol Genet 19(10):1873–1882
44. Janke C, Beck M, Stahl T, Holzer M, Brauer K, Bigl V, Arendt T (1999) Phylogenetic diversity of the expression of the microtubule-associated protein tau: implications for neurodegenerative disorders. Mol Brain Res 68(1–2):119–128
45. Jeffrey M, Piccardo P, Ritchie DL, Ironside JW, Green AJ, McGovern G (2015) A naturally occurring bovine tauopathy is geographically widespread in the UK. PLoS ONE 10(6):e0129499
46. Jiang Y, Xie M, Chen W, Talbot R et al (2014) The sheep genome illuminates biology of the rumen and lipid metabolism Science 344:1168–1173
47. Kametani F, Hasegawa M (2018) Reconsideration of amyloid hypothesis and tau hypothesis in Alzheimer's disease. Front NeuroSci 12:25
48. Kanaan NM, Pigino GF, Brady ST, Lazarov O, Binder LI, Morfini GA (2013) Axonal degeneration in Alzheimer's disease: when signaling abnormalities meet the axonal transport system. Exp Neurol 246:44–53
49. Knobloch M, Konietzko U, Krebs DC, Nitsch RM (2007) Intracellular Abeta and cognitive deficits precede beta-amyloid deposition in transgenic arcAbeta mice. Neurobiol Aging 28:1297–1306

50. Kosenko E, Tikhonova L, Alilova G, Urios A, Montoliu C (2020) The Erythrocytic Hypothesis of Brain Energy Crisis in Sporadic Alzheimer Disease: Possible Consequences and Supporting Evidence. *Journal of clinical medicine*, *9*(1), p.206
51. Koss DJ, Jones G, Cranston A, Gardner H, Kanaan NM, Platt B (2016) Soluble pre-fibrillar tau and β-amyloid species emerge in early human Alzheimer's disease and track disease progression and cognitive decline. Acta Neuropathol 132(6):875–895
52. Lau DH, Hogseth M, Phillips EC, O'Neill MJ, Pooler AM, Noble W, Hanger DP (2016) Critical residues involved in tau binding to fyn: implications for tau phosphorylation in Alzheimer's disease. Acta Neuropathol Commun 4(1):1–13
53. Lowe J, Ince P, Revesz T (2014) Neuropathology autopsy practice: Post-mortem examination in dementia. The Royal College of Pathologists. Unique document number G116
54. Maclean CJ, Baker HF, Ridley RM, Mori H (2000) Naturally occurring and experimentally induced β-amyloid deposits in the brains of marmosets (Callithrix jacchus). J Neural Transm 107(7):799–814
55. Mochizuki A, Tamaoka A, Shimohata A, Komatsuzaki Y, Shoji S (2000) Abeta42-positive non-pyramidal neurons around amyloid plaques in Alzheimer's disease. Lancet 355:42–43
56. Mondragon-Rodriguez S, Perry G, Luna-Munoz J, Acevedo-Aquino MC, Williams S (2014) Phosphorylation of tau protein at sites Ser(396–404) is one of the earliest events in Alzheimer's disease and Down syndrome. Neuropathol Appl Neurobiol 40:121–135
57. Morton AJ, Howland DS (2013) Large genetic animal models of Huntington's disease. J Huntington's Disease 2(1):3–19
58. Morton AJ (2018) Large-brained animal models of Huntington's disease: sheep. Huntington's Disease. Humana Press, New York, NY, pp 221–239
59. Morton AJ, Middleton B, Rudiger S, Bawden CS, Kuchel TR, Skene DJ (2020) Increased plasma melatonin in presymptomatic Huntington disease sheep (Ovis aries): Compensatory neuroprotection in a neurodegenerative disease? J Pineal Res 68(2):12624. .e
60. Nelson PT, Greenberg SG, Saper CB (1994) Neurofibrillary tangles in the cerebral cortex of sheep. Neurosci Lett 170(1):187–190
61. Nelson PT, Saper CB (1995) Ultrastructure of neurofibrillary tangles in the cerebral cortex of sheep. Neurobiol Aging 16(3):315–323
62. Nelson PT, Stefansson K, Gulcher J, Saper CB (1996) Molecular evolution of τ protein: implications for Alzheimer's disease. J Neurochem 67(4):1622–1632
63. Oakley H, Cole SL, Logan S et al (2006) Intraneuronal beta-amyloid aggregates, neurodegeneration, and neuron loss in transgenic mice with five familial Alzheimer's disease mutations: potential factors in amyloid plaque formation. J Neurosci 26:10129–10140
64. Oddo S, Caccamo A, Shepherd JD et al (2003) Triple-transgenic model of Alzheimer's disease with plaques and tangles: intracellular Abeta and synaptic dysfunction. Neuron 39:409–421

65. Pensalfini A, Albay III, Rasool R, Wu S, Hatami JW, Arai A, Margol H, Milton L, Poon S, Corrada WW, Kawas CH (2014) Intracellular amyloid and the neuronal origin of Alzheimer neuritic plaques. Neurobiol Dis 71:53–61
66. Regalado-Reyes M, Furcila D, Hernández F, Ávila J, DeFelipe J, León-Espinosa G (2019) Phospho-tau changes in the human CA1 during Alzheimer's disease progression. J Alzheimers Dis 69(1):277–288
67. Reid SJ, Mckean NE, Henty K, Portelius E, Blennow K, Rudiger SR, Bawden CS, Handley RR, Verma PJ, Faull RL, Waldvogel HJ (2017) Alzheimer's disease markers in the aged sheep (Ovis aries). Neurobiol Aging 58:112–119
68. Ricciarelli R, Fedele E (2017) The amyloid cascade hypothesis in Alzheimer's disease: it's time to change our mind. Curr Neuropharmacol 15(6):926–935
69. Dumbell R, Solbakk A, Ropstad E, Haraldsen IRH (2014) Effects of inhibition of gonadotropin releasing hormone secretion on the response to novel objects in young male and female sheep. Psychoneuroendocrinology, 40, pp.130–139
70. Rodriguez-Callejas JD, Fuchs E, Perez-Cruz C (2016) Evidence of tau hyperphosphorylation and dystrophic microglia in the common marmoset. Front Aging Neurosci 8:315
71. Rosen RF, Farberg AS, Gearing M, Dooyema J, Long M, Anderson P, Davis-Turak DC, Coppola J, Geschwind G, Paré DH, Duong TQ (2008) Tauopathy with paired helical filaments in an aged chimpanzee. J Comp Neurol 509(3):259–270
72. Sani S, Traul D, Klink A, Niaraki N, Gonzalo-Ruiz A, Wu CK, Geula C (2003) Distribution, progression and chemical composition of cortical amyloid-β deposits in aged rhesus monkeys: similarities to the human. Acta Neuropathol 105(2):145–156
73. Sarasa M, Pesini P (2009) Natural non-transgenic animal models for research in Alzheimer's disease. Curr Alzheimer Res 6(2):171–178
74. Sasaguri H, Nilsson P, Hashimoto S, Nagata K, Saito T, De Strooper B, Hardy J, Vassar R, Winblad B, Saido TC (2017) APP mouse models for Alzheimer's disease preclinical studies. EMBO J 36(17):2473–2487
75. Sawiak SJ, Perumal SR, Rudiger SR, Matthews L, Mitchell NL, McLaughlan CJ, Bawden CS, Palmer DN, Kuchel T, Morton AJ (2015) Rapid and progressive regional brain atrophy in CLN6 Batten disease affected sheep measured with longitudinal magnetic resonance imaging. *PloS one*, *10*(7), p.e0132331
76. Scheffer S, Hermkens DM, van der Weerd L, de Vries HE, Daemen MJ (2021) Vascular Hypothesis of Alzheimer Disease: Topical Review of Mouse Models. Arterioscler Thromb Vasc Biol 41(4):1265–1283
77. Sharma G, Huo A, Kimura T, Shiozawa S, Kobayashi R, Sahara N, Ishibashi M, Ishigaki S, Saito T, Ando K, Murayama S (2019) Tau isoform expression and phosphorylation in marmoset brains. J Biol Chem 294(30):11433–11444
78. Skene DJ, Middleton B, Fraser CK, Pennings JL, Kuchel TR, Rudiger SR, Bawden CS, Morton AJ (2017) Metabolic profiling of presymptomatic Huntington's disease sheep reveals novel biomarkers.

Sci Rep 7(1):1–16

79. Smolek T, Madari A, Farbakova J, Kandrac O, Jadhav S, Cente M, Brezovakova V, Novak M, Zilka N (2016) Tau hyperphosphorylation in synaptosomes and neuroinflammation are associated with canine cognitive impairment. J Comp Neurol 524(4):874–895
80. Sparks DL, Schreurs BG (2003) Trace amounts of copper in water induce β-amyloid plaques and learning deficits in a rabbit model of Alzheimer's disease. *Proceedings of the National Academy of Sciences*, *100*(19), pp.11065–11069
81. Stylianaki I, Komnenou AT, Posantzis D, Nikolaou K, Papaioannou N (2019) Alzheimer's disease-like pathological lesions in an aged bottlenose dolphin (Tursiops truncatus). *Veterinary Record Case Reports*, *7*(1)
82. Sun HL, Chen SH, Yu ZY, Cheng Y, Tian DY, Fan DY, He CY, Wang J, Sun PY, Chen Y, Tan CR (2020) Blood cell-produced amyloid-β induces cerebral Alzheimer-type pathologies and behavioral deficits. *Molecular Psychiatry*, pp.1–10
83. Sündermann F, Fernandez MP, Morgan RO (2016) An evolutionary roadmap to the microtubule-associated protein MAP Tau. *BMC Genomics*, *17*(1), p.264
84. Tabira T, Chui DH, Kuroda S (2002) Significance of intracellular Abeta42 accumulation in Alzheimer's disease. Front Biosci 7:a44–a49
85. Takaichi Y, Chambers JK, Takahashi K, Soeda Y, Koike R, Katsumata E, Kita C, Matsuda F, Haritani M, Takashima A, Nakayama H (2021) Amyloid β and tau pathology in brains of aged pinniped species (sea lion, seal, and walrus). *Acta Neuropathologica Communications*, *9*(1), pp.1–15
86. Tenreiro S, Eckermann K, Outeiro TF (2014) Protein phosphorylation in neurodegeneration: friend or foe? Front Mol Neurosci 7:42
87. Tsunoda K, Yamamoto Y, Akiya Y, Sato K, Rajbhandary HB, Van Son H, Loc CB (1998) Apolipoprotein E polymorphism in sheep. Biochem Genet 36(11–12):395–405
88. Uno H, Alsum PB, Dong S, Richardson R, Zimbric ML, Thieme CS, Houser WD (1996) Cerebral amyloid angiopathy and plaques, and visceral amyloidosis in aged macaques. Neurobiol Aging 17(2):275–281
89. Usenovic M, Niroomand S, Drolet RE, Yao L, Gaspar RC, Hatcher NG, Schachter J, Renger JJ, Parmentier-Batteur S (2015) Internalized tau oligomers cause neurodegeneration by inducing accumulation of pathogenic tau in human neurons derived from induced pluripotent stem cells. J Neurosci 35(42):14234–14250
90. Wirths O, Multhaup G, Bayer TA (2004) A modified beta-amyloid hypothesis: intraneuronal accumulation of the beta-amyloid peptide—the first step of a fatal cascade. J Neurochem 91:513–520
91. Zhai R, Rizak J, Zheng NA, He X, Li Z, Yin Y, Su T, He Y, He R, Ma Y, Yang M (2018) Alzheimer's disease-like pathologies and cognitive impairments induced by formaldehyde in non-human primates. Curr Alzheimer Res 15(14):1304–1321

92. Zhao L (2020) 2020 Alzheimer's disease facts and figures. *Alzheimers Dement.*, *16*, pp.391–460. DOI:10.1002/alz.12068

Figures

Figure 1

Immunohistochemistry of brain cortex of a very old sheep using the anti-phospho tau antibody AT8. A; Numerous NFTs are visible in the insular cortex and olfactory tract of a 21 year old sheep (sheep #P1), primarily within layer III (arrow). The regions enclosed by boxes are shown in B & C. B; An example of a NFT with phosphorylated tau aggregates visible within the cell soma and neuronal processes. C; An example of a NFT with phosphorylated tau confined to the cytoplasm and a single process. Scale bars represent 300μm (A) or 50μm (B, C).

Figure 2

Immunohistochemistry of sheep brain using the anti-Aβ-42 antibody ab12267. A; Numerous diffuse Aβ plaques are visible within the parietal cortex of a sheep 16 years of age (sheep #P2). B; An example of a diffuse Aβ plaque in the entorhinal cortex of a sheep >5 years of age (sheep #5). C & D; An example of positive intracellular cytoplasmic labelling of large neurons (arrows) in the pons of a sheep >5 years old (sheep #6). The section has been counterstained so nuclei are stained blue. Scale bars represent 500μm (A) or 50μm (B-D).

Figure 3

Immunohistochemistry of sheep brain using the anti-Aβ-42 antibody mOC64. A; Intracellular cytoplasmic staining of neurons is clearly visible as brown deposit within the entorhinal cortex (layers II and III) of a sheep >5 years of age (sheep #3). The region enclosed by the box is shown in B. B; The neuronal nuclei (nucleolus: arrowhead, nucleus: solid arrow) are clearly defined but non-labelled, as labelling is confined to the cytoplasm (open arrow). C; Intracellular cytoplasmic labelling of pyramidal neurons (layer V) within the entorhinal cortex of a sheep >5 years old (sheep #5). The region enclosed by the box is shown in D. D; Immunopositive staining is present in the cytoplasm and nuclei (arrows), and neurites (arrow heads). The

section has been counterstained so nuclei are stained blue. Scale bars represent 200μm (A & C) or 50μm (B & D).

Figure 4

Immunohistochemistry of sheep brain (pons) using anti-Aβ-42 antibodies. A, A'; An example of ab12267 antibody labelling of small vessels (arrows) in a sheep >5 years of age (sheep #10). B, B'; An example of mOC64 antibody labelling of small vessels (arrows) in a sheep >5-years of age (sheep #6). The section has been counterstained so nuclei are stained blue. Scale bars represent 200μm (A & B) or 50μm (A', B').

Figure 5

Pre-neurofibrillary tangles identified using the anti-phospho-tau antibody AT8. A; An example of a pre-neurofibrillary tangle (arrow) where the soma is homogenously immunoreactive and the nuclei exhibit speckled staining. B & C; Two examples of pre-neurofibrillary tangles (arrows) in the cell soma with nuclei that are clearly defined but unlabelled and neuritic compartments that appear speckled (arrows). Examples of non-labelled neurons are indicated in each panel (arrowheads). Scale bars represent 50μm (A-C). The section has been counterstained so nuclei are stained blue.

Figure 6

Immunohistochemistry of the CA3 region of sheep hippocampus. A; Labelling of neuronal processes within the substratum radiatum of the CA3 region of the hippocampus in a 1-2 year-old sheep is seen after immunostaining using the anti-phospho-tau S396 antibody (sheep #16). B; Labelling of both soma and neuronal processes in the CA3 region of the hippocampus in a 1-2 year-old sheep using the anti-pan-tau antibody DAKO0024 (sheep #16). C; Immunolabelling of the soma and neuronal processes using the Aβ-42 antibody, mOC64 within the CA3 region of the hippocampus of a sheep >5 years of age (sheep #6). Scale bars represent 200μm (A-C).

Figure 7

Immunohistochemistry using the anti-phospho-tau antibody, AT8, identified diffuse plaque-like regions not typical of AD tau pathology. A & B; An example of a small discrete positive region, with no other staining present in the surrounding tissue (sheep #4). The region enclosed by the box in A is shown in B. C & D; An example of a relatively large, intensely stained region that exhibits intra-cellular labelling, extracellular labelling, and non-labelled neurons (arrowheads) (sheep #5). The region enclosed by the box in C is shown in D. The section has been counterstained so nuclei are stained blue. Scale bars represent 200μm (A & C) or 50μm (B & D).

Figure 8

Differences in the average number of AT8 positive diffuse plaque-like regions between different brain regions and age groups of sheep. Graphical data are presented as mean ± S.E.M. Different letters ($^{a\text{-}d}$) indicate significant differences ($p<0.05$), shared letters indicate no significant differences. There was a significant interaction ($p<0.001$) between age and brain region on the number of AT8 positive regions identified. (PC; parietal cortex, Hipp & EC; hippocampus and entorhinal cortex).

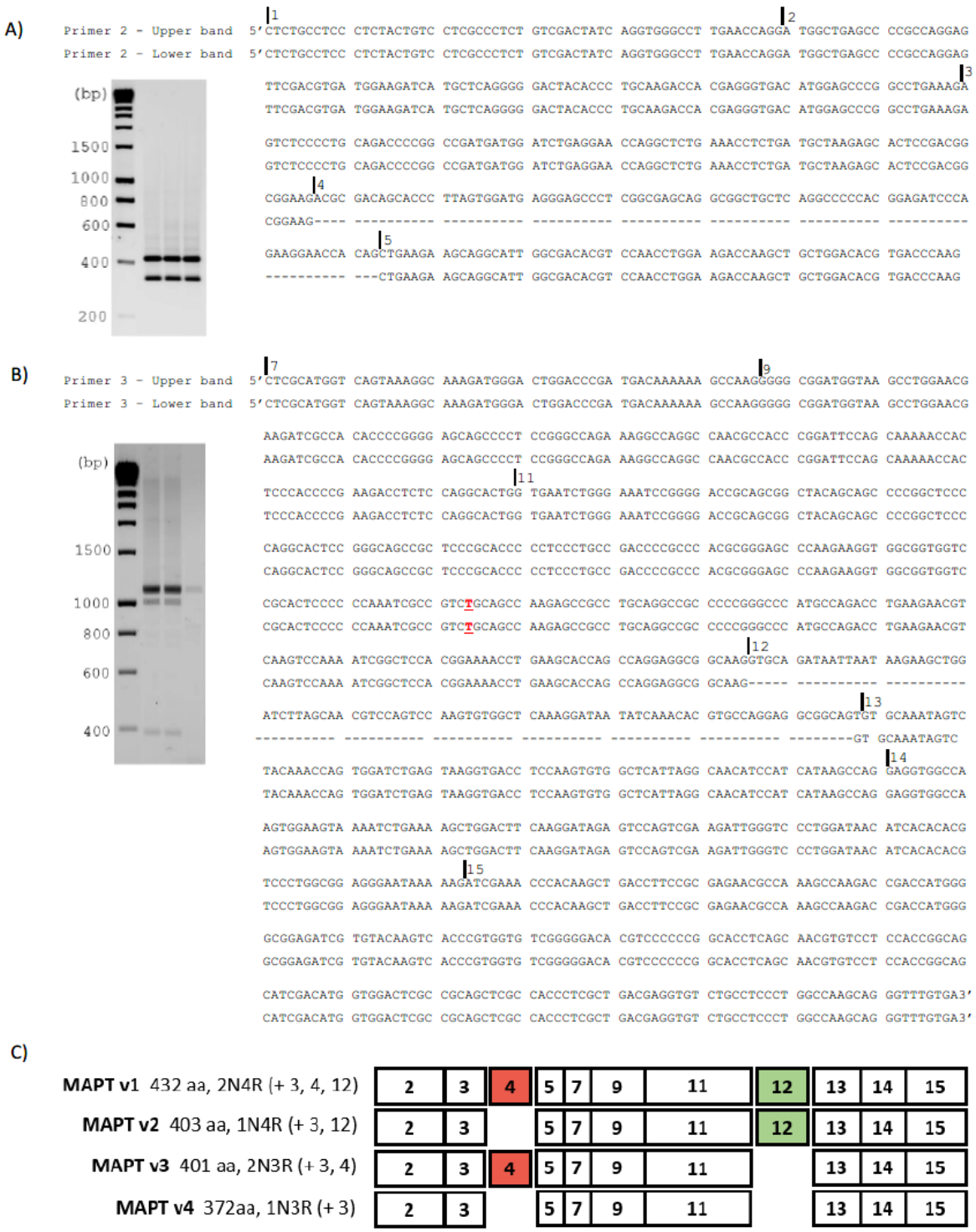

Figure 9

PCR cloning sequence analysis of ovine tau transcripts. A; Primer pair 2 spanning exons 1-7, confirms the splicing of exon 4. B; Primer pair 3 spanning exons 7-15, confirms the splicing of exon 12. Underlined nucleotide bases highlighted in red identify where nucleotides differ from those of the NCBI Predicted *Ovis aries* MAPT transcript, variant X1, XM_027974371.1. (bp; base pairs). C; The translated exons of the four central nervous system ovine MAPT isoforms identified in this study. The four transcripts, with 3(3R)

and 4(4R) microtubule binding repeat regions result from the alternative splicing of exons 4 and 12. Exons are described using standard exon nomenclature as detailed by Sündermann *et al.* [83].

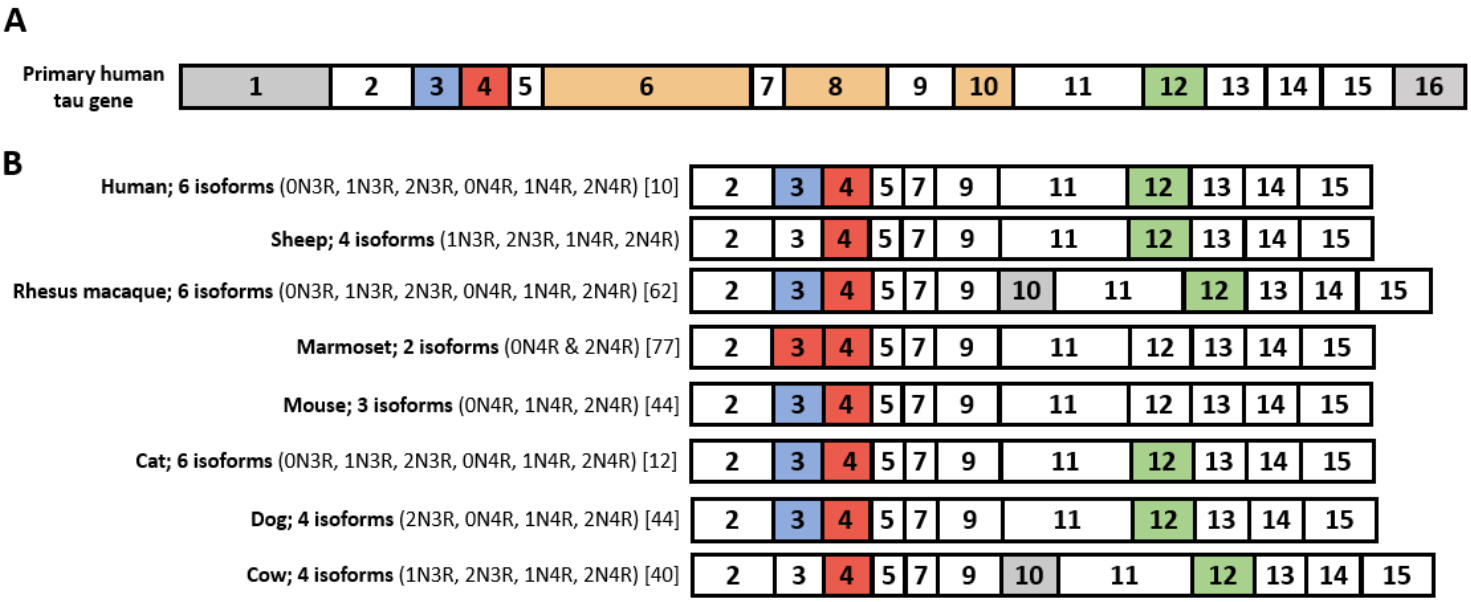

Figure 10

Diagrammatic representation of adult tau isoform expression in different species. Exons are described using standard exon nomenclature as detailed by Sündermann *et al.* [83]. Box sizes are representative of exon length. Grey boxes indicate exons that are transcribed but not translated. White boxes indicate constitutive exons that are translated. A; The complete human tau gene consists of 16 exons. Exon 1 is part of the promotor and is transcribed but not translated. Exons 6, 8 and 10 are specific to peripheral tau and are not transcribed in the brain. Exon 16 is transcribed but not translated. B; A comparison of CNS tau transcripts between humans and different animal species. Exons 1 and 16 are transcribed but not translated and have been omitted from the diagram. Coloured boxes (exons 3, 4 and 12) indicate exons that are alternatively spliced. In humans, exons 3, 4 and 12 are alternatively spliced, yielding six possible isoforms. Exon splicing and tau isoform expression differs between species. Note that exon 4 does not appear without exon 3. Note that exon 10 has been identified in some bovine and rhesus macaque brain tissue transcripts, although there is no evidence it is translated.

Figure 11

Western blot analysis using anti-phospho-tau antibody, S396. A; Representative western blot of three brain regions from three sheep >5 years of age (upper panel; sheep #1, #5 & #7), and three sheep 1-2

years of age (lower panel; sheep #15, #16 & #17). B; Average relative western blot signal intensities of all brain samples analysed using western blot. Data is presented as mean ± S.E.M. Different letters $^{(ab)}$ indicate significant differences. There was no statistically significant difference in mean intensity between brain regions, but there were statistically significant differences (p<0.001) between age groups (Hipp; hippocampus, EC; entorhinal cortex, FC; frontal cortex).

Supplementary Files

This is a list of supplementary files associated with this preprint. Click to download.

- OnlineResource1.pdf
- OnlineResource2Fig.S1.tif
- OnlineResource3.pdf